Journal of Neuroscience Research 86:1801–1811 (2008)

Whole-Brain Functional Magnetic Resonance Imaging Mapping of Acute Nociceptive Responses Induced by Formalin in Rats Using Atlas Registration-Based Event-Related Analysis

Yen-Yu I. Shih,[1,2] You-Yin Chen,[3] Chiao-Chi V. Chen,[2] Jyh-Cheng Chen,[4,5] Chen Chang,[2]* and Fu-Shan Jaw*

Institute of Biomedical Engineering, National Taiwan University, Taipei, Taiwan, Republic of China
Institute of Biomedical Sciences, Academia Sinica, Taipei, Taiwan, Republic of China
Department of Electrical and Control Engineering, National Chiao-Tung University, Hsinchu, Taiwan, Republic of China
Department of Biomedical Imaging and Radiological Sciences, National Yang-Ming University, Taipei, Taiwan, Republic of China
Department of Education and Research, Taipei City Hospital, Taipei, Taiwan, Republic of China

Nociceptive neuronal activation in subcortical regions has not been well investigated in functional magnetic resonance imaging (fMRI) studies. The present report aimed to use the blood oxygenation level-dependent (BOLD) fMRI technique to map nociceptive responses in both subcortical and cortical regions by employing a refined data processing method, the atlas registration-based event-related (ARBER) analysis technique. During fMRI acquisition, 5% formalin (50 μl) was injected into the left hindpaw to induce nociception. ARBER was then used to normalize the data among rats, and images were analyzed using automatic selection of the atlas-based region of interest. It was found that formalin-induced nociceptive processing increased BOLD signals in both cortical and subcortical regions. The cortical activation was distributed over the cingulate, motor, somatosensory, insular, and visual cortices, and the subcortical activation involved the caudate putamen, hippocampus, periaqueductal gray, superior colliculus, thalamus, and hypothalamus. With the aid of ARBER, the present study revealed a detailed activation pattern that possibly indicated the recruitment of various parts of the nociceptive system. The results also demonstrated the utilization of ARBER in establishing an fMRI-based whole-brain nociceptive map. The formalin induced nociceptive images may serve as a template of central nociceptive responses, which can facilitate the future use of fMRI in evaluation of new drugs and preclinical therapies for pain.

Key words: fMRI; pain; formalin; rat; atlas registration

Assessing nociception in small animals using imaging techniques has drastically increased in the last decade. Blood-oxygenation-level-dependent (BOLD) functional magnetic resonance imaging (fMRI) technique provides noninvasive, in vivo measurement of cerebral hemodynamics. Thus, it is a valuable approach in rapidly mapping central nociceptive responses of small animals. Several pain paradigms have been used to image brain activation, such as electrical stimulation-induced pain (Lowe et al., 2007) or chemical-induced nociception with, e.g., formalin (Tuor et al., 2000; Shah et al.,, 2005), capsaicin (Malisza and Docherty, 2001; Moylan Governo et al., 2006), and zymosan (Hess et al., 2007). Intense electrical stimulation tends to excite the Aβ, Aδ, and C fibers collectively (Chang and Shyu, 2001) and generates less specific activation patterns (Tuor et al., 2000). In contrast, formalin is a more specific nociceptive stimulus, insofar as it activates mainly C fibers (Tjolsen et al., 1992). Tuor et al. (2002) reported that formalin induced BOLD responses occurring primarily in the frontal cortical areas of α-chloralose-anesthetized rats. However, formalin-evoked BOLD responses in subcortical regions,

Contract grant sponsor: National Science Council, Taiwan, Republic of China; Contract grant number: NSC-94-2213-E-002-001; Contract grant number: NSC95-3112-B-001-009; Contract grant number: NSC95-3112-B-001-004.

*Correspondence to: Fu-Shan Jaw, Institute of Biomedical Engineering, National Taiwan University, No. 1, Sec. 4, Roosevelt Road, Taipei, Taiwan, Republic of China. E-mail: jaw@ntu.edu.tw or Chen Chang, Institute of Biomedical Sciences, Academia Sinica, No. 128, Sec. 2, Academia Road, Taipei, Taiwan, Republic of China.
E-mail: bmcchen@ibms.sinica.edu.tw

Received 26 August 2007; Revised 27 November 2007; Accepted 29 November 2007

Published online 21 February 2008 in Wiley InterScience (www.interscience.wiley.com). DOI: 10.1002/jnr.21638

such as caudate putamen, thalamus, hypothalamus, hippocampus, and periaqueductal gray were less well investigated, although these areas play an indispensable role in the pain matrix (Manning et al., 1994; Casey, 1999). To provide a better delineation of pain-evoked BOLD responses in the subcortical regions along with cortical areas, the current study aimed to depict the acute spatiotemporal patterns of BOLD activities in response to formalin-induced pain on a whole-brain scale.

Analyzing pain-evoked BOLD responses of both cortical and subcortical regions demands reliable data processing methods. In particular, the method used for extraction of BOLD signals from regions of interest (ROIs) can affect the results considerably. Manual ROI extraction requires reliable marking the margin of ROIs, but it is inevitably subjected to artificial errors. Therefore, computer-aided/atlas-based ROI extraction techniques are indispensable to generate reliable mapping results. To establish a BOLD signal map of formalin-induced pain responses on a whole-brain scale, the current study adopted a data analysis system that was developed in our laboratory to avoid problems associated with manual ROI extraction (Shih et al., 2007). The system, namely, the atlas registration-based event-related (ARBER) analysis technique, includes a standard rat brain reference system for spatial normalization and automatically correlates the temporal BOLD responses with the incidence of a stimulus. Additionally, the group response of the complicated pain processing networks could be shown in one map without collecting substantial rat brain MR images for making a normalized template.

The goal of the present study was to map BOLD fMRI-based whole-brain nociceptive responses with the aid of ARBER in data processing. To illustrate formalin-induced nociception clearly, invasive procedures were avoided to eliminate possible confounding variables. α-Chloralose was used for anesthesia to preserve better neurovascular coupling (Ueki et al., 1992). In the findings, BOLD signals were found in both cortical and subcortical areas following formalin injection, demonstrating an activation pattern covering various parts of the nociceptive system with the aid of ARBER.

MATERIALS AND METHODS

Subjects

In total 28 adult male Wistar rats (8–10 weeks old; weighing approximately 250–300 g; National Laboratory Animal Center, Taiwan) were used in the present study. The animals were kept in a well-maintained environment with 12:12-hour light-dark cycle and controlled humidity and temperature. Rats were triple-housed in plastic cages with free access to food and water. All experimental procedures were approved by the Institute of Animal Care and Utilization Committee at Academia Sinica, Taipei, Taiwan.

Animal Experiments

On the experiment day, each rat (n = 17) was anesthetized with α-chloralose given intraperitoneally at 70 mg/kg. The anesthetic was prepared by dissolving α-chloralose in 0.9% saline and 10% polyethylene glycol at 50–60°C on a stirring hotplate. The solution was cooled to 35–40°C before being injected. After anesthesia, the rat was fixed in a customerized head holder by two ear bars and an incisor fixer so as to minimize motion artifacts. The body temperature was maintained constant at 37°C using a warm-water blanket, and end-tidal CO_2 concentration was continuously monitored by a Datex-Ohmeda Capnomac Ultima respiration-ventilation monitor. After the rat was conditioned as described above, image acquisition was started. Details regarding MR image acquisition are provided in the section on Image Experiments.

After initial stimulation-free image acquisition, pain was induced by a single injection of 5% formalin (50 μl) into the left hindpaw. The injection was performed using a 250-μl microsyringe connected by 30-cm-long PE-50 tubing to a 30-G needle. Both the syringe and the tubing were filled with formalin. The needle was wiped clean with cotton prior to insertion into the hindpaw. Surgical tape was affixed to the hindpaw to secure the syringe needle during injection. The injected volume was carefully calibrated by repeatedly measuring the ejected formalin liquid.

An additional group of rats (n = 6) was used to record more detailed vital signs, including CO_2 concentration, heart rate, and electrocardiogram (EKG), as shown in Figure 1. The rats underwent identical experimental procedures for the same duration. Over the monitoring period, the averaged CO_2 concentrations ranged between 3% and 3.5%. No significant change was caused by formalin injection. The heart rate before formalin injection was 347.9 ± 10.3 bpm, and it was 373.1 ± 24 bpm afterward. Lead one EKG was recorded using a custom-built apparatus; the signal was bandpass filtered at 10–330 Hz and digitized at 512 Hz. EKG showed increased background noise compared with the initial state (Fig. 1B). Additional behavioral signs such as muscle twitches were also observed after formalin administration. Another separate group of animals (n = 5) were used for measures of arterial blood gases with a Osmetech OPTI blood gas analyzer. This group underwent identical anesthesia and treatment, except that additional cannulation was performed on the left femoral artery to sample the arterial blood parameters. Arterial blood gases before and after formalin injection were $PaCO_2$ 66.60 ± 8.44 and 55.60 ± 8.51 mmHg; PaO_2 100.40 ± 8.56 and 111.80 ± 8.35 mmHg; pH 7.29 ± 0.02 and 7.35 ± 0.05, respectively.

Image Experiments

For MRI experiments, images were captured with a 4.7-T Biospec 47/40 spectrometer. A 72-mm volume coil was used as the RF transmitter, and a 2-cm surface coil placed on the head was used as the receiver. A T_2-weighted scout image was taken in the midsagittal plane to localize the anatomical position by identifying the anterior commissure (bregma −0.8 mm). T_2-weighted template images (bregma −0.8 mm, −2.8 mm, −4.8 mm, and −6.8 mm) were acquired by using spin echo sequences with a repetition time (TR) of 4,000 msec, echo time (TE) of 80 msec, field of view (FOV) of 4 cm, slice thickness (SLTH) of 2 mm, number of excitations (NEX) of 2, and acquisition matrix of 256 × 128 (zero-filled to 256 × 256). Since the rat head was

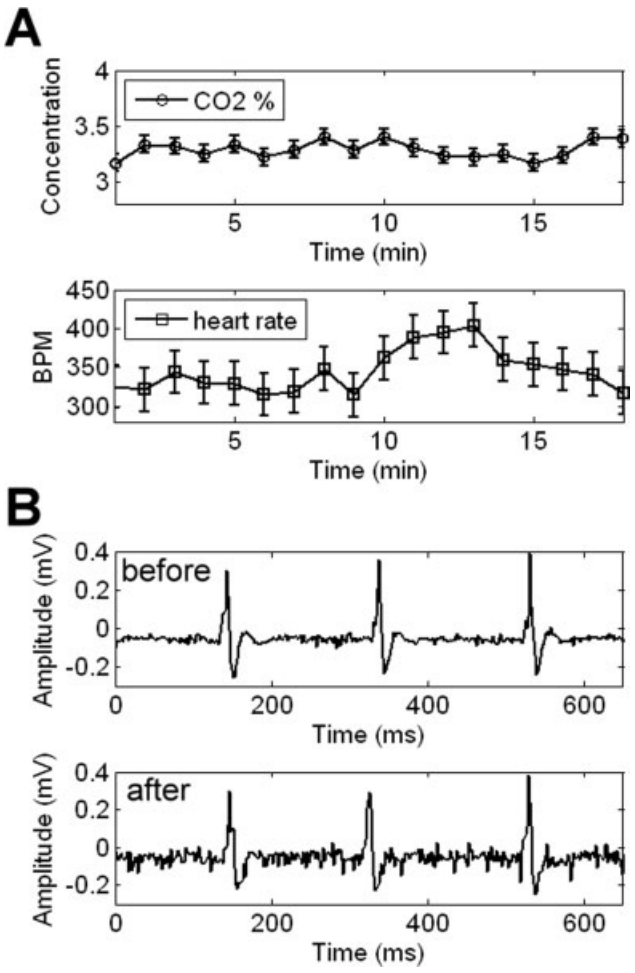

Fig. 1. Effects of formalin injection on the following physiological parameters: CO_2 concentration, heart rate, and EKG. **A:** CO_2 concentration and heart rate were continuously recorded for 18 min, with formalin injected at the beginning of the tenth min. The averaged CO_2 concentration ranged between 3% and 3.5% during the monitoring period and was not significantly affected by formalin injection. The heart rate before formalin injection was 347.9 ± 10.3 (mean ± SD) bpm and was 373.1 ± 24 bpm after. **B:** Lead-1 EKG before and after formalin injection. Background noise was increased following formalin treatment (bottom panel) compared with the initial state (top panel).

fixed firmly to the stereotaxic frame with two ear bars in an identified interaural line through the external auditory meatus, the image appeared to be horizontal. If rotation occurs, the stereotaxic frame in the magnetic bore was adjusted to correct angle until the scanned image showed no rotation. In the few cases of visible motion artifacts, the animal was remounted to the stereotaxic head holder. No gating to respiration was employed in the current study, because it may complicate the calculation of resting/stimulation duration. Forty-repetition gradient echo images were acquired at the same position of template images with a TR of 215 msec, TE of 20 msec, flip angle of 22.5°, FOV of 4 cm, SLTH of 2 mm, NEX of 2, acquisition matrix of 256 × 64 (zero-filled to 256 × 256), and temporal resolution of 27 sec. For event-related image acquisition, the first 20 consecutive frames were categorized as baseline images, and the remaining 20 were collected after formalin was injected into the hindpaw.

Data Analysis

BOLD MR images were analyzed with a custom-built ARBER analyzing interface. The major functions include MR-atlas coregistration, atlas-based ROI selection, and atlas-based spatial averaging. To improve the accuracy with which anatomical locations were determined, the MR images were registered with a digital atlas of the rat brain (Paxinos and Watson, 1998). The digital atlas was captured from the atlas PDF file using the snapshot tool in Adobe Acrobat 6.0 and then transformed into a 2D binary matrix in Matlab. Manual scaling and shifting operations were used to align the edges of fMRI and atlas images. Shifting represented translation of the images, and all the contents of the images were moved by the assigned pixel shift. A scaling factor was applied to transform the atlas image. In this process, bicubic transformation was performed in x and y directions to deal with the different resolutions between fMRI and atlas images. The registration was initially performed using a set of T_2-weighted template images. In addition to the edge of the image, important anatomical landmarks, such as ventricles and corpus collasum, were also used as references to achieve satisfactory registration. Gradient echo images were than fused with the atlas by identical spatial transform. Thus, the activated signals had a clear spatial reference after coregistration (Fig. 2). An automatic atlas-based ROI selection technique was then created by predefining the coordinates of each brain area in digital matrices. These coordinates composed the edge of each brain structure and generated a corresponding ROI (Fig. 2).

Dynamic cine analysis was used for a few animals to illustrate the spatiotemporal pattern of the acute formalin pain, the color-coded pixel values for each subimage were formed by subtracting the mean map of the baseline data, and the threshold was set as a 5% increase from the baseline. Background was omitted from the analysis by eliminating signals with lower intensity than the head tissue.

Correlation images were mapped by calculating correlation coefficients pixel-by-pixel to provide relativity between the activated responses and the stimulated paradigm as follows:

$$C(x,y) = \frac{\sum_{t=1}^{N}[P(x,y,t) - \mu_P(x,y)][R(t) - \mu_R]}{\sqrt{\sum_{t=1}^{N}[P(x,y,t) - \mu_P(x,y)]^2}\sqrt{\sum_{t=1}^{N}[R(t) - \mu_R]^2}}$$

where $R(t)$ is the function of input paradigm, $P(x,y,t)$ is the function of time activity curve, $\mu_P(x,y)$ is the mean of $P(x,y,t)$, and μ_R is the mean of $R(t)$. The temporal profile of each pixel was calculated with an OFF-ON paradigm model, and a correlation coefficient of $r = \pm 0.6$ was used as a threshold value. The activated pixels were labeled on the template images using hot and cold colors to code correlation coefficients ≥ 0.6 and ≤ -0.6, respectively.

The time-activity curves were created by averaging time courses from activated pixels in the ROIs, and only activation

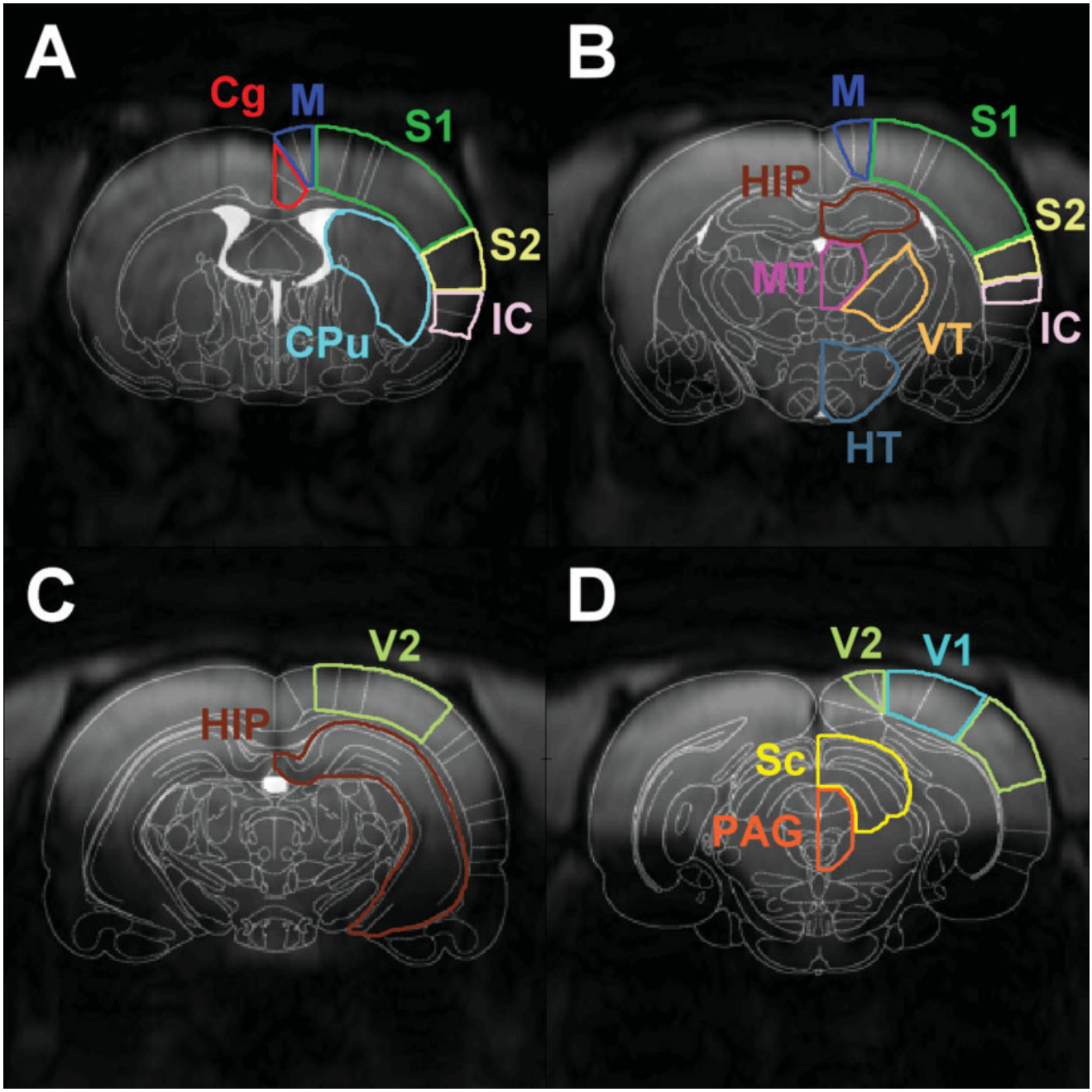

Fig. 2. T_2-weighted images were registered and fused with the rat atlas. These templates provided anatomical alignment and corresponding ROI selection. The four images correspond to 0.8 mm (**A**), 2.8 mm (**B**), 4.8 mm (**C**), and 6.8 mm (**D**) posterior to the bregma. [Color figure can be viewed in the online issue, which is available at www.interscience.wiley.com.]

of more than two pixels was considered a response. The 17 rat brain images were transformed into a rat atlas reference domain after the registration process. Incidence images were obtained by averaging the correlation coefficients of the number of subjects that exhibited an activation response. They represent the correlation maps of the activation group, in which a higher pixel value indicates a greater number of rat responses that are consistent with the stimuli. This method is less susceptible to group variations than when using *P* value maps. The incidence value of each pixel is the average of individual correlation coefficients and ranges from −1 to 1. In contrast, when using the *P* value map, subject data with a very high statistical power would distort the averaged results because there is no lower boundary for *t*-statistics.

The relative BOLD responses were compared before and after injection for each ROI. The preinjection response of a given ROI was calculated as the percentage difference of frames 11–20 relative to frames 1–10, and the postinjection response was measured from the percentage difference of frames 21–30 relative to frames 11–20. Only activated ROIs were included in the analysis per the descriptions provided above. Statistical analysis was based on the activated intensity (normalized from 0% to 100%). In each defined brain area, preinjection and postinjection responses were compared using paired *t*-tests, where $P < 0.05$ was considered to indicate a significant difference.

RESULTS

Seventeen rats underwent α-chloralose anesthesia and formalin injections followed by imaging studies. The scanned images were carefully checked for rotation and motion. No rotation or motion was seen in any of the images, and ARBER was then applied for all data analyses.

Formalin-Evoked BOLD Responses: A Single Case Illustration

Figure 3 presents pixelwise time-series images and stimulus-response correlation images of a rat following formalin injection. Figure 3A–D shows 20 dynamic images (27 sec each) that depict BOLD signal changes at four anterior-posterior levels for 10 min after a formalin injection. The color in each image indicates the intensity of above-threshold BOLD signals (5%) subtracted from the baseline values on a pixel-by-pixel basis within the ROIs.

Formalin-induced nociception caused increases in the BOLD signals in areas including primary somatosensory cortex (S1), bed nucleus of stria terminalis (BST), cingulate cortex (Cg), motor cortex (M), secondary somatosensory cortex (S2), hippocampus (HIP), medial thalamus (MT), secondary visual cortex (V2), and superior colliculus (Sc), among which areas S1 and Sc exhibited sustained activation. Regions where activation occurred first but was only transient included the BST, MT, HIP, and V2. Cg and adjacent motor cortices exhibited late-activated responses. BOLD activation appeared to involve both hemispheres even though the stimulus was applied unilaterally. No negative BOLD signals were observed with the threshold set at 5%, indicating that a decrease in event-related signals was not obvious under the experimental conditions used.

Spatial Distribution of Formalin-Evoked BOLD Responses

The colored regions in the correlation maps in Figure 3E revealed activation areas of the same rat whose activation pattern corresponded to the OFF-ON stimulus paradigm. The following structures showed event-related responses: Cg, M, BST, S1, S2, insular cortex (IC), primary visual cortex (V1), V2, caudate putamen (CPu), HIP, periaqueductal gray (PAG), Sc, MT, ventrolateral thalamic group (VLT), and hypothalamus (HT).

Figure 4 shows the averaged incidence images. The correlation coefficients of 17 formalin-treated rats were averaged on a pixel-by-pixel basis in the ROIs, and the averaged means were color coded. Figure 4 shows that, within cortical regions, the activation of the hindlimb area of S1, Cg, and M coincided with the nociceptive stimulus. The averaged values were lower in the superior part of these areas, possibly because of the influence of susceptibility artifacts caused by local magnetic field inhomogeneity near air-tissue interfaces. In the subcortical regions, the BOLD responses in HIP and Sc corresponded to the off and on status of the stimulus. However, the activation in CPu and thalamus observed in the case shown in Figure 3 diminished after averaging the responses.

The increases in BOLD signals at each time point were expressed as percentage difference relative to the baseline value, defined as the mean signal intensity for 9 min before formalin injection. An ROI was considered to be activated if it contained at least two activated pixels postinjection, where a pixel was considered to be activated if the BOLD signal increased by at least 5% relative to the baseline value. Table I lists how many of the 17 rats showed activation in each given ROI following formalin injection (e.g., 13 rats exhibited activation in the ipsilateral Cg).

Temporal Patterns of Formalin-Evoked BOLD Responses

Figure 5 shows the time-activity curves of each ROI over the 40 time points (i.e., the 18-min imaging period). For each ROI, the signal intensity at each time point corresponds to the mean increase in the BOLD signal of the activated subjects. The patterns of response increases were similar across the ROIs. The signals tended to increase immediately after formalin injection, reach a maximum within 3 min, and remain elevated for at least 9 min. The time taken for the BOLD signal intensity to reach its peak may reflect the time required to increase maximally the regional cerebral blood flow due to neuronal activation (Fox and Raichle, 1986; Fox et al., 1988). The signal increases ranged between 3% and 9% relative to the baseline values. No significant difference in intensity or activation onset was observed between the two hemispheres.

DISCUSSION

The current study established a BOLD fMRI-based whole-brain nociceptive map using the ARBER analyzing technique. It was found that formalin-induced nociceptive processing recruited hemodynamic activity in both cortical and subcortical regions during the 10 min postinjection. The cortical activation was distributed over Cg, M, S1, S2, IC, V1, and V2, and the subcortical activation involved CPu, HIP, PAG, Sc, MT, VLT, and HT. The activated responses tended to increase immediately following injection and remained elevated thereafter. Moreover, the responses in these regions coincided well with the occurrence of the nociceptive stimulus.

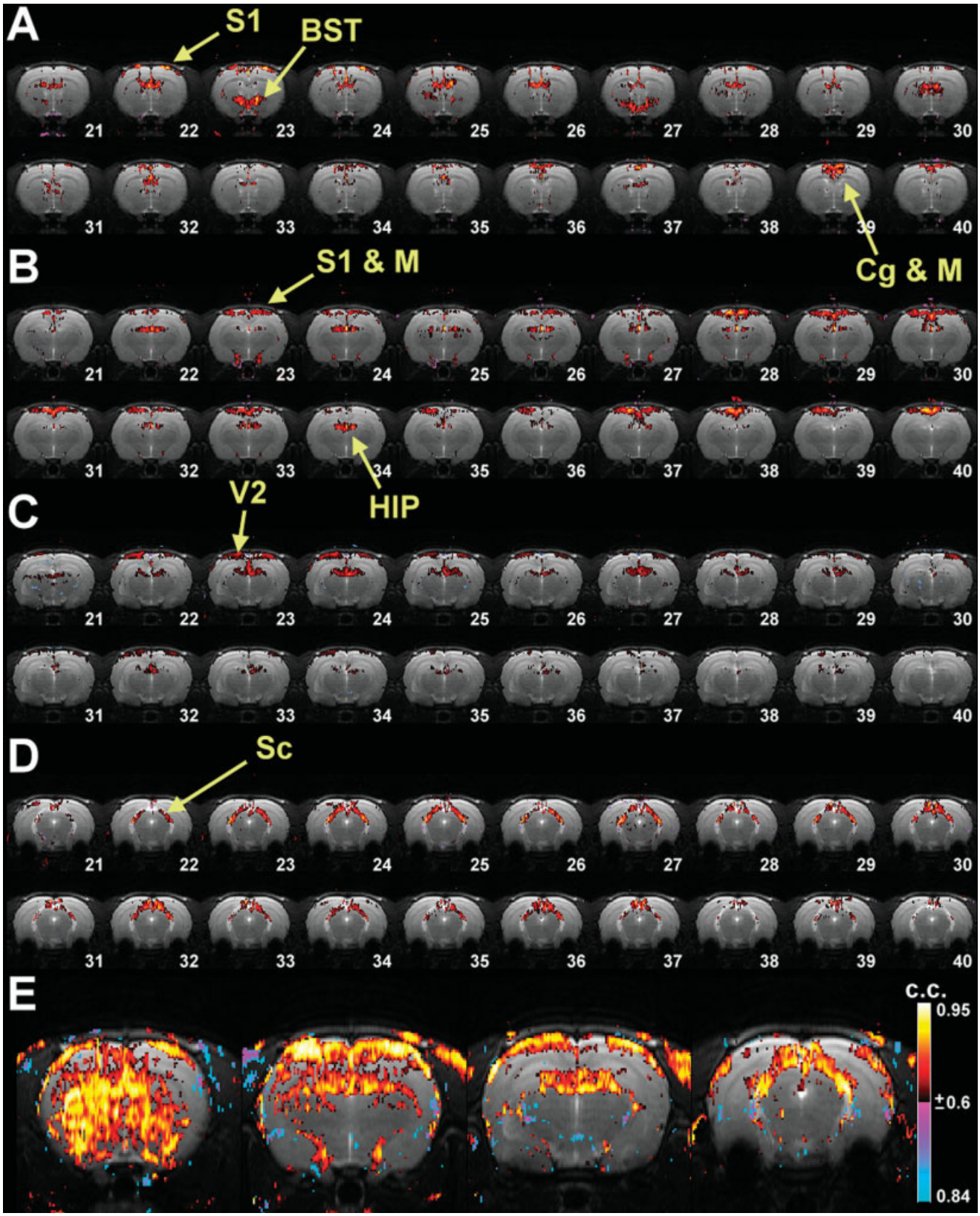

Fig. 3. Pixelwise time-series images and stimulus-response correlation maps of a rat following formalin injection into the left hindpaw. A–D show 20 dynamic images (27 sec each) that depict BOLD signal changes at four anterior-posterior levels for 10 min after the formalin injection. The pixel colors in each subimage indicate the intensity of above-threshold signals subtracted from the baseline values, with the threshold corresponding to a 5% increase relative to the baseline. Each series of images corresponds to 0.8 mm (**A**), 2.8 mm (**B**), 4.8 mm (**C**), and 6.8 mm (**D**) posterior to the bregma. **E:** The colored regions in these correlation maps revealed areas of the brain whose activation pattern corresponded to the OFF-ON stimulus paradigm. Event-related activations are indicated by hot and cold colors for correlation coefficients (C.C.) over 0.6 and under −0.6, respectively. [Color figure can be viewed in the online issue, which is available at www.interscience.wiley.com.]

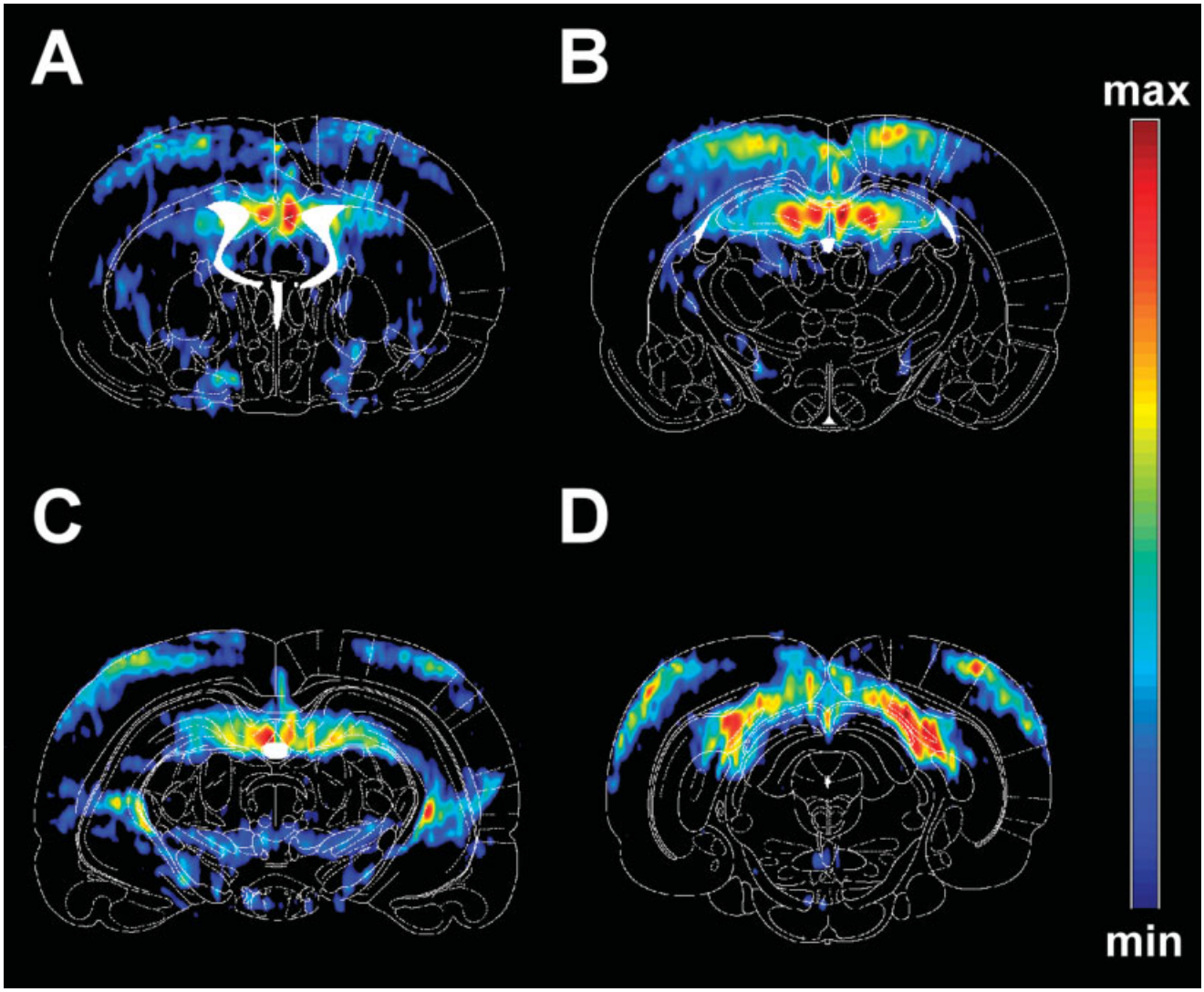

Fig. 4. Incidence images calculated by averaging the correlation coefficient maps for the 17 rats. Each correlation map was registered to the rat brain atlas before averaging. Strong activation was observed in the cortex and HIP. The minimal intensity for the activation images was set at 0.375 of the maximal intensity (i.e., the range of the displayed threshold in the images is defined by min = max × 0.375). Negative correlation coefficients were omitted from the analysis. The four images correspond to 0.8 mm (**A**), 2.8 mm (**B**), 4.8 mm (**C**), and 6.8 mm (**D**) posterior to the bregma. [Color figure can be viewed in the online issue, which is available at www.interscience.wiley.com.]

TABLE I. Number of Animals in Which Activation Was Detected for Each Brain Area*

	Cg	M	S1	S2	IC	V1	V2	Cpu	HIP	PAG	Sc	MT	VLT	HT
Ipsilateral	13	15	14	15	4	12	10	13	17	8	14	14	5	12
Contralateral	15	14	15	14	4	9	7	14	17	8	15	11	7	13

*The total number of rats was 17, and a response was considered present only when an ROI contained more than two activated pixels. Cg, cingulate cortex; M, motor cortex, S1, primary somatosensory cortex; S2, secondary somatosensory cortex; IC, insular cortex; V1, primary visual cortex; V2, secondary visual cortex; CPu, caudate putamen; HIP, hippocampus; PAG, periaqueductal gray; Sc, superior colliculus; MT, medial thalamus; VLT, ventrolateral thalamic group; HT, hypothalamus.

ARBER is a stereotaxically concordant analysis system for MR image registration and analysis. It is particularly useful in analyzing spatiotemporal BOLD signals of multiple brain regions. It greatly reduces artificial errors arising from ROI selection and thus generates a more reliable map representing formalin-induced pain signals. The group response of the formalin-induced nociception could also be shown in one incidence image, making it

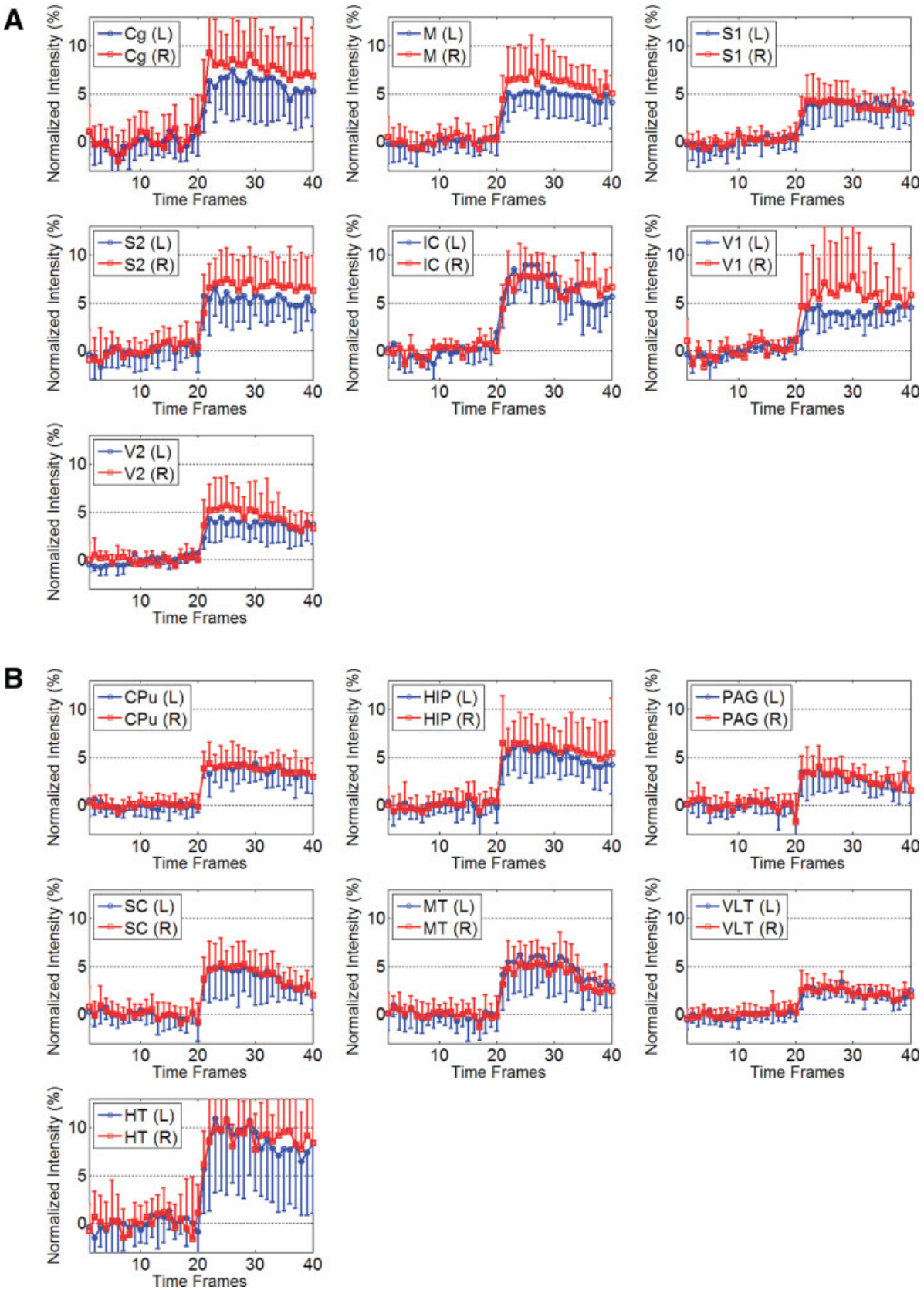

Fig. 5. Averaged time-activity curves in activated brain areas (n = 17). Formalin was injected at time point 21. Each brain area was separated into ipsilateral and contralateral regions. The signal intensities are expressed as percentages relative to baseline values. Mean and SD values are shown for cortical (**A**) and subcortical (**B**) areas. L, left; R, right. [Color figure can be viewed in the online issue, which is available at www.interscience.wiley.com.]

no longer necessary to evaluate the spatial distribution of activation from a single-subject image as in the previous reports (Tuor et al., 2000; Shah et al., 2005). Schwarz et al. (2006) recently created a distribution map of the tissue class that serves as an MRI template to facilitate the localization of brain functional effects. Although this method allows a closer alignment of MR images, it was not easy to be used by researchers who do not have access to such a substantial database. Moreover, ARBER provides sufficient resolution along all three axes (Shih et al., 2007), because it is based on the conventional rat brain atlas (Paxinos and Watson, 1998). This feature is not available in the atlas developed by the Schwartz group.

The distribution of whole-brain BOLD responses reveals the multifaceted nature of central nociceptive networks. Nociceptive pathways including spinothalamic, spinoreticular, spinohypothalamic, and spinobulbar tracts appeared to participate in formalin-induced nociception (McMahon and Koltzenburg, 2005). Activation in VLT and MT, which are the direct termination sites of the spinothalamic and spinoreticular pathways, may indicate the involvement of these two major nociceptive tracts that carry nociceptive information to the central nervous system (Craig, 2003). Signal increases in the cortical regions such as S1, S2, and Cg that are the subsequent terminations of the two nociceptive pathways further support this view. Additionally, the spinobulbar tract also plays a role in this nociceptive transmission, because two critical regions that are directly terminated by this pathway (i.e., PAG and Sc) exhibited increased BOLD signal intensities. Surprisingly, the sensory-motor cortices were not activated in all animals (Table I). Two factors may explain this. First, BOLD fMRI studies intrinsically, inevitably suffer from a low contrast to noise ratio. Second, anesthetics may induce varying intersubject anesthesia and consequently different level of activation responses.

The BOLD activation pattern of formalin-induced pain also suggests the involvement of the autonomic affective system, endogenous antinociception, and motor system. Activation of HT, BST, and HIP may indicate the participation of the autonomic affective circuitry. HT, a major termination of the spinohypothalamic pathway, is the key structure for governing autonomic endocrine responses to stressful conditions such as pain (Giesler et al., 1994). BST and HIP are two important limbic structures that are involved in the integration of visceral responses induced by emotion-arousing stimuli. The activation of these regions, possibly along with the Cg activation as mentioned above, implies the affective aspect of nociception.

V1 and V2 also showed event-related activation, which should not have resulted from visual stimulation, because the lighting conditions were constant throughout the experiment (Fig. 4). To the best of our knowledge, formalin-induced signals in visual cortices have not been found previously in fMRI studies. The activation of V1 and V2 is intriguing. Studies have shown a high density of opiate receptors within these regions, which suggests that their activation may initiate the endogenous antinociceptive system to regulate nociceptive processing (Lewis et al., 1983). The activation of PAG may also participate in such modulation (Martin et al., 1996). Another component that may be involved is the motor system, as suggested by BOLD signal increases in M and CPu, which might be driven by the excitation of sensory and cingulate cortices (Chudler et al., 1993; Lorenz et al., 2003). The increased motor activity may account for the increased background noise in EKG signals following formalin injection as can be seen in Figure 1B.

The current study reported a bilateral pattern for brain areas that were activated by formalin-induced nociception. Bilateral activation caused by unilateral nociceptive stimuli has been reported in many previous studies. For instance, BOLD formalin experiments conducted by Tuor et al. (2000) showed activation occurring bilaterally in the Cg, M, S1, and S2. Shah et al. (2005) used a similar paradigm of formalin pain to map responses mainly in subcortical regions and found bilateral activation in the nucleus accumbens, CPu, PAG, HT, MT, and amygdala. Although the spinothalamic pathway is mainly considered a contralateral projection, bifurcation of the pathway also occurs (Dong et al., 1994; Millan, 1999). In addition, connections between two hemispheres might also account for the bilateral activation (Bramham et al., 1996; Sherman and Guillery, 1996; Zhang et al., 1996; Shin et al., 1997). Interestingly, unlike the case with formalin, electrical stimulation-induced pain appears to recruit mostly the activation of the contralateral somatosensory cortex, as revealed by Lowe et al. (2007). It remains to be elucidated why unilateral electrical stimulation causes contralateral responses, whereas unilateral formalin injection induces bilateral activation. We speculate that the difference in the type of sensory fibers recruited by each of the stimuli might underlie the activation disparity.

Anesthesia is often required in animal fMRI studies to obtain reliable images. Thus, the influence of anesthetics is an important variable that should be taken into account when interpreting the results from such studies (Lindauer et al., 1993). The current study utilized α-chloralose for anesthesia, because it is widely acceptable for BOLD fMRI studies owing to its minimal suppression of neuronal activity (Ueki et al., 1992). Although it has been reported that α-chloralose may introduce variability to the hemodynamic responses in the late stage of anesthesia (Austin et al., 2003, 2005), such adverse effects were minimized in the current study by confining the scan time to within 1 hr. Furthermore, the effects of the α-chloralose given intraperitoneally last merely 1 hr or so, making it difficult to record the later phase of formalin pain (at least 30 min is needed for set up and collecting baseline responses). Although inhalant anesthetics such as isoflurane and halothane induce longer and more stable sedation, they have been reported to suppress brain hemodynamic activities (Alkire et al., 2000; Liu et al., 2004; Zhao et al., 2007). Other studies have combined a custom-built stereotaxic apparatus, muscle relax-

ants, and animal training techniques aimed at replacing anesthesia procedures, with the resultant brain responses possibly closely resembling those in fully conscious states (Peeters et al., 2001; Sicard et al., 2003). As expected, the BOLD signals were larger in these studies than under anesthetized conditions. However, it remains unclear whether the additional responses were due to the intended nociceptive stimuli or to stress and discomfort associated with confinement, noise generated from image scanning, and immobilization. Moreover, the use of muscle relaxants or conditioning training may cause less specific activation patterns and hence larger group variances. In addition, even though anesthesia usually suppresses brain responses and vascular activity, it is essential for fMRI nociceptive studies, because it not only minimizes the background noise associated with the experimental procedures but also reduces the suffering of animals. Although inclusion of only the early phase of formalin-induced pain is not as informative as studying the entire course, the acute period alone is worth investigation. It represents a continuous intense pain and corresponds to the stage showing the most manifest behavioral signs associated with pain. fMRI study of both acute and inflammatory phases of formalin-induced pain may become possible if suitable anesthetics are made available in the future, such as the method proposed by Weber et al. (2006).

Figure 3E shows slight activation in muscle. Significant blood pressure changes have been reported to cause nonspecific activation resulting from the increase of cerebral blood flow (Tuor et al., 2002). However, previous results demonstrated that injection of 5% 50 μl formalin into the left hindpaw would not significantly elevate the blood pressure, and the nonspecific BOLD change was not observed (Tuor et al., 2000, 2002; Shah et al., 2005). Furthermore, in Figure 3A–D, no activation in the muscles is observed, indicating that signal increases of muscles were less than 5%.

Nociception is a rather complicated modality that demands the use of observation tools with high temporal and spatial resolutions. fMRI is gradually accepted as a common technique for studying nociceptive mechanisms. Its ability to provide a macroscopic view of the brain nociceptive responses at a high spatial resolution is particularly advantageous. The present study used refined approaches to depict changes in the activities of central nociceptive pathways. A more detailed and specific activation pattern was observed, which possibly recruited various aspects of the nociceptive system. The results demonstrated that the ARBER analysis fMRI-based whole-brain nociceptive map may serve as a template of central nociceptive responses and facilitate the future use of fMRI in the evaluation of new drugs and preclinical therapies for pain.

ACKNOWLEDGMENTS

The authors acknowledge technical support from the Functional and Micro-Magnetic Resonance Imaging Center and the Molecular-Genetic Imaging Core, which are supported by the National Research Program for Genomic Medicine of the National Science Council, Taiwan, Republic of China (grants NSC95-3112-B-001-009 and NSC95-3112-B-001-004).

REFERENCES

Alkire MT, Haier RJ, Fallon JH. 2000. Toward a unified theory of narcosis: brain imaging evidence for a thalamocortical switch as the neurophysiologic basis of anesthetic-induced unconsciousness. Conscious Cognit 9:370–386.

Austin VC, Blamire AM, Grieve SM, O'Neill MJ, Styles P, Matthews PM, Sibson NR. 2003. Differences in the BOLD fMRI response to direct and indirect cortical stimulation in the rat. Magn Reson Med 49:838–847.

Austin VC, Blamire AM, Allers KA, Sharp T, Styles P, Matthews PM, Sibson NR. 2005. Confounding effects of anesthesia on functional activation in rodent brain: a study of halothane and alpha-chloralose anesthesia. Neuroimage 24:92–100.

Bramham CR, Southard T, Sarvey JM, Herkenham M, Brady LS. 1996. Unilateral LTP triggers bilateral increases in hippocampal neurotrophin and trk receptor mRNA expression in behaving rats: evidence for interhemispheric communication. J Comp Neurol 368:371–382.

Casey KL. 1999. Forebrain mechanisms of nociception and pain: analysis through imaging. Proc Natl Acad Sci U S A 96:7668–7674.

Chang C, Shyu BC. 2001. A fMRI study of brain activations during non-noxious and noxious electrical stimulation of the sciatic nerve of rats. Brain Res 897:71–81.

Chudler EH, Sugiyama K, Dong WK. 1993. Nociceptive responses in the neostriatum and globus pallidus of the anesthetized rat. J Neurophysiol 69:1890–1903.

Craig AD. 2003. Pain mechanisms: labeled lines versus convergence in central processing. Annu Rev Neurosci 26:1–30.

Dong WK, Chudler EH, Sugiyama K, Roberts VJ, Hayashi T. 1994. Somatosensory, multisensory, and task-related neurons in cortical area 7b (PF) of unanesthetized monkeys. J Neurophysiol 72:542–564.

Fox PT, Raichle ME. 1986. Focal physiological uncoupling of cerebral blood flow and oxidative metabolism during somatosensory stimulation in human subjects. Proc Natl Acad Sci U S A 83:1140–1144.

Fox PT, Raichle ME, Mintun MA, Dence C. 1988. Nonoxidative glucose consumption during focal physiologic neural activity. Science 241:462–464.

Giesler GJ Jr, Katter JT, Dado RJ. 1994. Direct spinal pathways to the limbic system for nociceptive information. Trends Neurosci 17:244–250.

Hess A, Sergejeva M, Budinsky L, Zeilhofer HU, Brune K. 2007. Imaging of hyperalgesia in rats by functional MRI. Eur J Pain 11:109–119.

Lewis ME, Pert A, Pert CB, Herkenham M. 1983. Opiate receptor localization in rat cerebral cortex. J Comp Neurol 216:339–358.

Lindauer U, Villringer A, Dirnagl U. 1993. Characterization of CBF response to somatosensory stimulation: model and influence of anesthetics. Am J Physiol 264:H1223–H1228.

Liu ZM, Schmidt KF, Sicard KM, Duong TQ. 2004. Imaging oxygen consumption in forepaw somatosensory stimulation in rats under isoflurane anesthesia. Magn Reson Med 52:277–285.

Lorenz J, Minoshima S, Casey KL. 2003. Keeping pain out of mind: the role of the dorsolateral prefrontal cortex in pain modulation. Brain 126:1079–1091.

Lowe AS, Beech JS, Williams SC. 2007. Small animal, whole brain fMRI: Innocuous and nociceptive forepaw stimulation. Neuroimage 35:719–728.

Malisza KL, Docherty JC. 2001. Capsaicin as a source for painful stimulation in functional MRI. J Magn Reson Imag 14:341–347.

Manning BH, Morgan MJ, Franklin KB. 1994. Morphine analgesia in the formalin test: evidence for forebrain and midbrain sites of action. Neuroscience 63:289–294.

Martin WJ, Hohmann AG, Walker JM. 1996. Suppression of noxious stimulus-evoked activity in the ventral posterolateral nucleus of the thalamus by a cannabinoid agonist: correlation between electrophysiological and antinociceptive effects. J Neurosci 16:6601–6611.

McMahon SB, Koltzenburg M. 2005. Wall and Melzack's textbook of pain: New York: Churchill Livingstone.

Millan MJ. 1999. The induction of pain: an integrative review. Prog Neurobiol 57:1–164.

Moylan Governo RJ, Morris PG, Prior MJ, Marsden CA, Chapman V. 2006. Capsaicin-evoked brain activation and central sensitization in anaesthetised rats: a functional magnetic resonance imaging study. Pain 126:35–45.

Paxinos G, Watson C. 1998. The rat brain in stereotaxic coordinates: San Diego: Academic Press.

Peeters RR, Tindemans I, De Schutter E, Van der Linden A. 2001. Comparing BOLD fMRI signal changes in the awake and anesthetized rat during electrical forepaw stimulation. Magn Reson Imag 19:821–826.

Schwarz AJ, Danckaert A, Reese T, Gozzi A, Paxinos G, Watson C, Merlo-Pich EV, Bifone A. 2006. A stereotaxic MRI template set for the rat brain with tissue class distribution maps and co-registered anatomical atlas: application to pharmacological MRI. Neuroimage 32: 538–550.

Shah YB, Haynes L, Prior MJ, Marsden CA, Morris PG, Chapman V. 2005. Functional magnetic resonance imaging studies of opioid receptor-mediated modulation of noxious-evoked BOLD contrast in rats. Psychopharmacology 180:761–773.

Sherman SM, Guillery RW. 1996. Functional organization of thalamocortical relays. J Neurophysiol 76:1367–1395.

Shih YY, Chen YY, Chen JC, Chang C, Jaw FS. 2007. ISPMER: integrated system for combined PET, MRI, and electrophysiological recording in somatosensory studies in rats. Nucl Instrum Methods A (in press).

Shin HC, Oh S, Jung SC, Park J, Won CK. 1997. Differential modulation of short and long latency sensory responses in the SI cortex by IL-6. Neuroreport 8:2841–2844.

Sicard K, Shen Q, Brevard ME, Sullivan R, Ferris CF, King JA, Duong TQ. 2003. Regional cerebral blood flow and BOLD responses in conscious and anesthetized rats under basal and hypercapnic conditions: implications for functional MRI studies. J Cereb Blood Flow Metab 23:472–481.

Tjolsen A, Berge OG, Hunskaar S, Rosland JH, Hole K. 1992. The formalin test: an evaluation of the method. Pain 51:5–17.

Tuor UI, Malisza K, Foniok T, Papadimitropoulos R, Jarmasz M, Somorjai R, Kozlowski P. 2000. Functional magnetic resonance imaging in rats subjected to intense electrical and noxious chemical stimulation of the forepaw. Pain 87:315–324.

Tuor UI, McKenzie E, Tomanek B. 2002. Functional magnetic resonance imaging of tonic pain and vasopressor effects in rats. Magn Reson Imag 20:707–712.

Ueki M, Mies G, Hossmann KA. 1992. Effect of alpha-chloralose, halothane, pentobarbital and nitrous oxide anesthesia on metabolic coupling in somatosensory cortex of rat. Acta Anaesthesiol Scand 36:318–322.

Weber R, Ramos-Cabrer P, Wiedermann D, Van Camp N, Hoehn M. 2006. A fully noninvasive and robust experimental protocol for longitudinal fMRI studies in the rat. Neuroimage 29:1303–1310.

Zhang HQ, Murray GM, Turman AB, Mackie PD, Coleman GT, Rowe MJ. 1996. Parallel processing in cerebral cortex of the marmoset monkey: effect of reversible SI inactivation on tactile responses in SII. J Neurophysiol 76:3633–3655.

Zhao F, Jin T, Wang P, Kim SG. 2007. Isoflurane anesthesia effect in functional imaging studies. Neuroimage 38:3–4.